Manifestations of Different El Nino types in the Dynamics of Extratropical Stratosphere

Tatiana Ermakova (taalika@mail.ru)
Russian State Hydrometeorological University https://orcid.org/0000-0003-0808-2226
Alexander Pogoreltsev
Russian State Hydrometeorological University: Rossijskij gosudarstvennyj gidrometeorologiceskij universitet
Sergei Smyshlyaev
Russian State Hydrometeorological University: Rossijskij gosudarstvennyj gidrometeorologiceskij universitet
Andrey Koval
Saint Petersburg State University: Sankt-peterburgskij gosudarstvennyj universitet
Wen Chen
CAS Institute of Atmospheric Physics: Institute of Atmospheric Physics Chinese Academy of Sciences
Ke Wei
CAS Institute of Atmospheric Physics: Institute of Atmospheric Physics Chinese Academy of Sciences

Research Article

Keywords: El Nino type, planetary waves, travelling waves, dynamics of stratosphere

Posted Date: March 30th, 2021

DOI: https://doi.org/10.21203/rs.3.rs-344873/v1

Abstract

The behavior of planetary wave with zonal wave number 1 (PW1) at the heights of middle and upper stratosphere during different El Nino types has been considered. The sets of 5 winters have been chosen for each El Nino type using the table of available extended Multivariate El Nino Southern Oscillation (ENSO) Index values and index for identifying different types of El Nino Modoki events. Comparing planetary wave response and residual circulation under various conditions caused by Modoki I, II, and canonical El Nino, it has been revealed identical features associated with any of this type. The activity of travelling waves has been presented at three latitudes (2.5, 27.5, and 62.5) of Northern Hemisphere to follow the changes in behavior of waves. Travelling waves determined at 2.5°N latitude during every El Nino type have similar wave activity distribution despite the different location of SST anomaly. The standing waves activity at 27.5°N latitude during Modoki II type is similar to this activity during canonical one. This similarity disappears at lower latitudes, where wave amplitudes every canonical winter do not distinguish each other greatly especially standing and westward propagating waves.

Introduction

El Nino Southern Oscillation (ENSO) is the phenomenon, which has three phases and irregular cycle of a coupled ocean-atmosphere interaction. Over the years, El Nino – the “warm” phase of ENSO phenomenon – has become very popular due to free access to scientific information and community-wide discussion. The considerable part of the population in tropical regions is familiar with this ‘coupled’ climate event. The reason is extreme weather, which is observed during this ENSO phase. Fish population die or migrate these years since the normal upwelling is absent and coastal ecosystem changes. Increased convection above warmer Pacific brings raised precipitation. This results in heavy rains and devastating floods. While South America suffers from floodwaters, severe droughts occur in Indonesia and Australia (Ward et al. 2016; Nobre et al. 2017; Chung and Power 2017; Iqbal and Hassan 2018; Foley and Kelman 2020;).

Stronger El Nino events interfere as global atmospheric circulation via remote impacts. The movement of atmospheric heat sources directed to the East lead to uncommon winter weather at higher altitudes. Sea Surface Temperature (SST) and pressure anomalies can affect even the stratosphere trough the teleconnections. The Aleutian low tends to deepen and goes southward during El Nino. This leads to the strengthening of wave activity flux upward to stratosphere and the weakening of polar vortex (Garfinkel and Hartmann 2008; Ineson and Scaife 2009; Bell et al. 2009; Garfinkel et al. 2010; Smith et al. 2010; Smith and Kushner 2012; Rao and Ren 2016a). Despite scientists’ efforts to improve the understanding of the ENSO’s phenomenon through new technologies, techniques, and approaches, many questions around. Most studies dedicated to different phases of ENSO influence on planetary waves behavior concentrate on equatorial-trapped Rossby-Gravity and extratropical planetary waves (Chen et al., 2002; Kim and Kim, 2002; Dima and Wallace, 2007; Rakhman et al. 2017) or planetary waves at the heights of stratosphere (Garcıa-Herrera et al., 2006; M. Taguchi and D. Hartmann, 2006; Garfinkel and Hartmann, 2007; Ermakova et al. 2019), ignoring the eastward traveling waves.

According to Pacific location of SST anomalies, El Nino phase can be divided into central Pacific (CP or “Modoki” - a Japanese word meaning “similar but different”) (Larkin and Harrison 2005; Ashok et al. 2007; Yu

and Kim 2011) and eastern Pacific (EP or canonical) (Larkin and Harrison 2005; Hurwitz et al. 2014; Domeisen et al. 2019). It is noted that there is more substantial and rapid response of Aleutian low to eastern Pacific El Nino type in contrast to central Pacific (Yu and Kim 2011; Sung et al. 2014). The polar stratosphere exhibits a more pronounced warming and, as a consequence, the polar vortex weakening during EP, while there is no consensus on CP mostly due to differences in its definition.

In order to distinguish two types of El Niño, several methods and indices have been suggested. The El Niño type can be determined by comparing the values of the Niño3 and Niño4 indices (Kug et al. 2009; Yeh et al. 2009). The SST anomalies, furthermore, in the tropical southeastern Pacific (150–90°W, 0°–10°S) represent El Niño Modoki events as well (Qu and Yu 2014). Some of indexes are based on the empirical orthogonal function analysis of the SST anomalies (Ashok et al. 2007; Kao and Yu 2009; Di Lorenzo et al. 2010; Takahashi et al. 2011).

Considering the impacts of Modoki El Nino expressed in rainfall in southern China during boreal autumn (Wang and Wang 2013), the CP can be classified into Modoki I and Modoki II. The separation principle includes not only rainfall anomalies but also the spatial–temporal evolutions of SST anomalies. The origin of positive SST anomaly locates in the equatorial central Pacific and in the subtropical northeastern Pacific for Modoki I and Modoki II, respectively.

Obviously, the three types of El Nino send different signal about the extreme weather phenomena in the troposphere. To analyze this signal the behavior of planetary waves at different latitudes: 2.5°N, 27.5°N and 62.5°N has been examined. Equatorial planetary waves, e.g. Kelvin wave, are excited by convective heating in the equatorial region (Chapman and Lindzen 1970; Tsuda and Kato 1989; Forbes et al. 1997). They induce meridional circulation that is why latitude of 2.5°N has been included in the present study. Latitude of 27.5°N allows demonstrating variability of travelling planetary waves, while at higher latitudes these waves are obfuscated by the standing and quasi-stationary waves (Pogoreltsev et al. 2009). The extratropical low-frequency westward propagating normal atmospheric modes are well observed at higher mid-latitudes (e.g. 62.5°N) since their amplitudes are the greatest here (Salby 1984; Fedulina et al. 2004). The question is whether the thermodynamic differences are observed under Modoki I, Modoki II and canonical El Nino conditions in the stratosphere? This paper is concerned primarily with this problem.

Data And Methods

Motivated by development of index which identifies the types of El Nino events (Wang et al. 2017), the estimations of thermodynamical stratospheric features during different El Nino winter conditions in the Northern Hemisphere are presented. The JRA-55 (https://jra.kishou.go.jp/JRA-55/index_en.html) Reanalysis covering the period from 1958 to present day is employed to analyze the behavior of planetary waves under Modoki I, Modoki II and canonical conditions.

Using the table of available extended Multivariate ENSO Index (MEI) values (https://psl.noaa.gov/enso/mei.ext/table.ext.html; https://psl.noaa.gov/enso/mei/data/meiv2.data) and results obtained by Wang et al. 2017, the following sets of winters have been chosen: 1963/64, 1979/80, 1987/88, 1992/93, and 2002/03 – Modoki I winters, 1968/69, 1977/78, 1991/92, 1994/95, and 2009/10 – Modoki II winters, 1965/66, 1972/73, 1982/83, 1997/98, and 2015/16 – canonical El Nino type winters.

Positive values in Table 1, magnitudes greater than 0.5, indicate El Nino warm phase of the ENSO. ‘The warmest’ winters are 1972/73, 1982/83, 1997/98 and 2015/16 (canonical type). “The coldest” ones are 1979/80, 1992/93 and 2002/03 (Modoki I type). Winter 1979/80 shows the smallest values of MEI index values, just late autumn months have magnitudes slightly greater than 0.5. This winter can be rather referred to neutral phase, while other ENSO indexes (The Oceanic Niño Index (ONI) and Nino3.4) demonstrate positive SST anomaly during winter months and Wang et al. identify this winter as Modoki I type of El Nino.

Table 1
Bimonthly MEI index values.

YEAR	JulAug	AugSep	SepOct	OctNov	NovDec	DecJan	JanFeb	FebMar	MarApr
1963/64	**0,91**	**1,06**	**1,11**	**1,07**	**0,97**	**0,93**	**0,73**	0,25	-0,35
1965/66	**1,73**	**1,73**	**1,42**	**1,52**	**1,73**	**1,68**	**1,53**	**1,21**	**0,89**
1968/69	-0,34	0,20	**0,62**	**0,73**	**0,66**	**0,76**	**1,04**	**1,03**	**0,94**
1972/73	**2,21**	**2,07**	**1,88**	**1,84**	**2,01**	**2,02**	**1,76**	**1,30**	**0,74**
1977/78	**0,75**	**0,72**	**0,83**	**1,01**	**1,11**	**0,94**	**0,85**	**0,90**	**0,57**
1979/80	0,44	0,38	0,24	**0,52**	**0,65**	0,35	0,19	0,41	**0,59**
1982/83	**2,02**	**1,81**	**1,93**	**2,28**	**2,48**	**2,57**	**2,74**	**2,68**	**2,79**
1987/88	**1,48**	**1,23**	**1,13**	**0,85**	**0,75**	**0,59**	0,31	0,19	-0,01
1991/92	0,42	**0,62**	**1,09**	**1,17**	**1,29**	**1,70**	**1,59**	**1,72**	**1,98**
1992/93	0,08	**0,50**	**0,81**	**0,73**	**0,78**	**0,83**	**0,93**	**0,78**	**0,98**
1994/95	**0,84**	**1,06**	**1,47**	**0,99**	**0,87**	**0,77**	0,48	0,14	0,18
1997/98	**2,20**	**2,17**	**2,01**	**2,06**	**2,03**	**2,23**	**2,43**	**2,27**	**2,55**
2002/03	**0,97**	**0,84**	**0,79**	**0,76**	**0,86**	**0,80**	**0,62**	**0,53**	-0,08
2009/10	**0,52**	0,39	**0,56**	**1,05**	**0,96**	**0,93**	**1,28**	**1,31**	0,49
2015/16	**1,92**	**2,21**	**2,11**	**1,88**	**1,90**	**1,94**	**1,81**	**1,31**	**1,33**

The amplitudes of zonal harmonics with zonal wave numbers 1 in the geopotential height are presented in Fig. 1. A strong variability with time that is caused by nonlinear interaction of this wave with zonal mean flow, the so-called stratospheric vacillations, is evident (Holton and Mass 1976; Pogoreltsev 2007). Another reason of observed variability is the interference of stationary planetary waves with travelling waves, for instance, the interference of the SPWs and free atmospheric oscillations or the normal atmospheric modes (Salby 1984).

Traveling planetary waves have been extracted using a space-time spectral analysis of the geopotential height fields based on the complex Morlet wavelet transform (Torrence and Compo 1998). It is examined the wave with zonal wave number m = 1. The extraction method was described in Pogoreltsev et al. (2002) and (2009). It should be noted that the separation of the geopotential height oscillations into the westward and eastward propagating components is to some extent artificial. Two waves with the same period and amplitudes that propagate westward and eastward can be presented as a standing wave.

Analyzing the activity of stationary planetary wave with zonal wave number one (SPW1) it is worth considering its impact on the mean flow. However, in the momentum and energy equations, the wave sources of momentum and heat are compensated by advective momentum and heat fluxes (Charney and Drazin 1961). To fill this gap, the alternative approach can be applied. It is the calculation of the transformed Eulerian mean circulation (TEM, Andrews and McIntyre 1976) that has been used in the present study. The essence of this method is the consideration of the so-called residual mean meridional circulation (RMC), which is a combination of eddy and advective mean transport.

Results

The amplitudes of SPW1 during different El Nino types are presented in Fig. 1. Maximum amplitude peaks greater than 2500 meters arise in January 1964, February 1988, December 2002 (referred to as Modoki I), in the end of December 1994, December 2009, and January 2010 (Modoki II), December 1982, February 2016 (canonical El Nino). In both cases (Fig. 1c and Fig. 1o, respectively), when the observed greatest amplitudes occur in February, the maximum MEI values achieve of about 2 and appear to be in the summer. The substantial SPW1 amplitudes in December during Modoki both types can be also related to MEI values, which are of about unit and have the highest magnitude in early autumn months. Winters 1963/64 and 1987/88 have similar MEI values distribution and in both cases there is PW1 amplification, which is not so dramatic, in the beginning of cold season: in the first case – middle of November, in the second case – end of November. December 1982 (canonical El Nino) doesn't follow this pattern. Short time intervals of increased wave activity are found during three types of El Nino in different winter months.

The observed temporal variability of the amplitudes and phases of the zonal harmonics is due to the superposition of the variability of SPWs, which can be explained by a change in the conditions of their propagation from the troposphere and/or the nonlinear interaction with the mean flow, and by the presence of traveling and standing planetary waves (PWs) in the reanalysis data. Traveling (propagating to the East and to the West of the PWs) and standing planetary waves, in turn, are also nonstationary. As a result, the situation is rather complicated and the complex Morlet transform is used to estimate the variability of their amplitudes and phases. The technique of waves' division into traveling to the East and West, and the further recalculation of the results obtained to distinguish standing waves, are described in Pogoreltsev et al. (2009). The amplitudes of standing PW1 and traveling to the East and to the West at 2.5°N are shown in the Figs. 2–4, respectively. Despite the different origin of SST anomaly, some winters have a very similar wave activity distribution (penetration) of both the period and maximum amplitude magnitudes. In Fig. 2 there is a calm standing wave behavior during winters with Modoki I type (1979/80, 1992/93), Modoki II type (1977/78, 1994/95), and canonical type (1972/73, 1982/83): the most active waves with 3-4-day periods and amplitude peaks do not reach 25 meters. In contrast one should note the winters (1997/98 – canonical type and 2002/03 – Modoki I), when the standing PW1 with 6-day period is active in January and February. The amplitude values are of about 25 meters in February. Paying attention to traveling waves, eastward planetary waves with periods greater than 10 days and amplitudes 2–4 meters are observed every winter during Modoki I and canonical types (Fig. 3). These waves occur not so often and they are less sustainable. Traveling westward waves with different periods are active up to mid-January and in March during Modoki I excluding winter 1992/93 (Fig. 4). The same pattern holds in winter of Modoki II type in 2009/10. The 4-day and 6-day waves have the largest amplitudes, which exist in all El Nino types. The standing and traveling waves have been determined at 27.5°N

(not presented) and 62.5°N (Fig. 5–7). The standing waves at 27.5°N during Modoki I winters are mainly with the periods of 10-day and greater. They have amplitude peaks in December and February. The 8-day standing waves occur during Modoki II and canonical El Nino, but in the first case the 15-20-day waves have the strongest amplitudes. They start disappearing in February and the amplitudes become roughly equal to 20 meters. It should be noted that calm March without large amplitudes of any waves features every winter. The waves traveling to the East at this latitude do not have distinctive features for Modoki I and II El Nino types. There is no any wave activity in the March and even in February (1965/66, 1972/73, and 1997/98). The activity of westward propagating waves at 27.5°N is minimal in the second half of January and in the first half of February except winter 1965/66. Evidently for the standing waves at 62.5°N it is difficult to find characteristic features to mark any El Nino type (Fig. 5). The reason is likely in different stratospheric processes and zonal flows that influence waves' distribution and make them behave in a certain way. In canonical El Nino winters (Fig. 6f-j), there is a two-week pause while any eastward wave activity is absent, at the beginning of January. Figure 7 (k-o) demonstrates that in canonical El Nino, the westward waves with shorter periods (from 8 to 15 days) are observed at the beginning of winter. In the end of January or in February, waves with longer periods (15–20 days) occur. There is the only 10-day or 15-day waves for long time interval (of about two months) during Modoki II El Nino event.

Traveling planetary waves (the normal atmospheric modes, ultra-fast Kelvin wave, etc.), unlike atmospheric tides, do not have permanent sources, therefore they exist (observed in the results of wavelet analysis) in the form of bursts of wave activity at certain periods that are not tied to a specific time interval (Salby 1984). Therefore, to compare the wave activity of traveling planetary waves induced by different types of El Nino events, the amplitude wavelet spectra have been averaged over 5 months (from November to March). Figures 8 and 9 demonstrate the standing, eastward, and westward waves averaged over boreal winter seasons during different El Nino types at 2.5°N and 62.5°N, respectively. It is obvious that both amplitudes of nonmigrating diurnal tide (Fig. 8a, b, c) and amplitudes of Kelvin waves (Fig. 8d, e, f) are overstated all years up to 1979 regardless of El Nino type, most likely due to lack of satellite data in reanalysis data. There are two peaks of amplitudes over 8 meters after diurnal tides in Modoki I and canonical events, while there is the only one in Modoki II. The distribution of eastward propagating waves has no common features in various El Nino types considering wave amplitudes and periods. The amplitudes of diurnal migrating tide propagating to the West (Fig. 8g, h, i) are the greatest during Modoki II. It should be noted that this overstating of diurnal tides is observed in amplitudes at 27.5°N (not presented here) as well but only in the standing waves and it is the highest during Modoki II event. During this type of El Nino all westward propagating waves have their amplitudes of about 20 meters, while in Modoki I and canonical El Nino types 10-day wave dominates and the amplitude of about 30 meters is observed. The difference in the highest amplitudes is observed in standing waves at 62.5°N (Fig. 9a, b, c). The magnitudes of amplitudes do not exceed 200 meters in Modoki II event (Fig. 9b), but they reach 250 meters in Modoki I event (Fig. 9a) and the 20-day wave occur with the amplitude of 300 meters in 2015/16 (canonical type, Fig. 9c). The 16-day wave dominates among the traveling to the East with the amplitude from 20 to 50 meters and of about 100 meters in 2002/03 (Modoki I, Fig. 9d). Such strong amplitudes (92 meters) belong as well to 13-day eastward propagating waves (canonical El Nino, Fig. 10f) in 1982/83 and 2015/16.

Planetary waves provide wave fluxes of heat and / or long-lived atmospheric species. To account for these fluxes, it is usually considered the so-called residual meridional circulation (Andrews et al. 1987), which is the

Brewer-Dobson circulation at the heights of the stratosphere-mesosphere. The observed variability of this circulation, as well as its climatic variability, can significantly clarify the changes in the thermal regime and ozone content in the Polar Regions during SSW events and / or depending on the ENSO, quasi-biennial oscillation (QBO), and Madden-Julian oscillation phases.

Taking into account the amplitude overstating at 2.5°N and altitude limitation of JRA-55, the residual circulation has been calculated using MERRA2 (The Modern-Era Retrospective analysis for Research and Applications, https://gmao.gsfc.nasa.gov/reanalysis/MERRA-2/) reanalysis data for every December (Fig. 11, 12, and 13, left panels) and January (Fig. 10, 11, and 12, right panels). The distribution of residual circulation in these two months should be enough, allowing for that the wave activity begins in December and January, to assume that any dependence upon El Nino type is there. December in 1987/88 and 1992/93 shown in Fig. 10 (mid and bottom left panels) differ from one another by strength of flow and its direction especially over Pole despite the same QBO phase and previous ENSO phase as well, in both cases it was positive. In contrast, the residual circulation in December 1992 is similar to that in December 2002 (Fig. 10, top left panel) while in the latter case the opposite QBO phase is observed and neutral previous ENSO phase. However, the MEI values in fall months have identical meaning of about 0.8 in these years, and they are greater in 1987. The residual circulation in December in Modoki II event (Fig. 11 left panels) looks very similar to one in 2002 and 1992 (Modoki I), but the flow is noticeably weaker at the altitude of 50–60 km at mid-latitudes. It should be noted the strong reverse flow in this height region at 35°N directed to the South in December 1991. In January of Modoki II El Nino type (Fig. 11 right panels) the flows become very similar to those observed in 2003 and 1993 despite different QBO phases and ENSO conditions in previous summer. There is absolutely different pattern in December of canonical El Nino (Fig. 12 left panels). Every circulation differs from another be the strength of flows and their direction. The differences are smoothed out in January (Fig. 12 left panels), but still are evident.

Conclusion

The behavior of planetary wave with zonal wave number 1 (PW1) in the middle and upper stratosphere during different El Nino types has been considered. Comparing planetary wave response and residual circulation under various conditions caused by Modoki I, II, and canonical El Nino, it has been done an attempt to reveal identical features associated with any of this type. Obviously, in the extratropical stratosphere, there is weak interannual variability under conditions of the canonical El Niño type. At lower latitudes, it is extremely difficult to distinguish a particular El Nino type in the stratosphere, taking into account only the penetration of planetary waves. Often several winters demonstrate a similar behavior of the PW1 under conditions of different El Niño types.

The PW1 behavior during Modoki I and II types of El Nino is similar and can be connected with MEI values distribution, i.e. the time of the highest index magnitudes can provide the time interval of amplitude amplification. The PW1 behavior during canonical conditions differs every examined winter but available data do not enough to judge the reasons. Travelling waves determined at 2.5°N latitude during every El Nino type have similar wave activity distribution despite the different location of SST anomaly. It allows to conclude that SST anomaly is not the only cause of equatorial waves' behavior. The standing waves activity at 27.5°N latitude during Modoki II type is similar to this activity during canonical one. This similarity disappears at

62.5°N latitude that is more evident at the figures with the amplitude wave spectra averaged over cold season. It can be explained by the fact, that commonly Modoki events are not as strong as the canonical ones and are less controlled by equatorial ocean-atmosphere coupling (Capotondi et al. 2015).

It is difficult to estimate the amplitude wave spectra averaged over 5 months of cold season since the amplitudes of nonmigrating diurnal tides and Kelvin waves are found to be overestimated all years up to 1979. General shape of curves taking into account maximal amplitudes of standing and traveling waves in Modoki I and canonical winters look similar. Modoki II differs by smaller amplitudes and smoother curves. This difference especially reveals at the mid-latitudes, where wave amplitudes every canonical winter do not distinguish each other greatly especially standing and westward propagating waves.

Residual circulation in every considered winter has no identical features especially in November and December. Taking into account the various origin location of SST anomaly, reflected in MEI values and time, when this anomaly is begun to observe, it is possible to conclude that this information as initial is not enough. This observation suggests that the other troposphere-stratosphere processes of equal importance interfere directly or via teleconnections influencing the propagation of planetary waves into the stratosphere.

In the present study the only PW1 has been considered, while the smaller harmonics can show interesting results with the similar analysis. Strong amplitudes with magnitudes more than 1000 meters of stationary planetary waves with zonal wave number 2 (SPW2) are observed in the same winters as for SPW1, some of them even in the same months. Considering SPW2, the wave activity in March attracts attention. Amplitudes of more than 500 meters are common in March during Modoki I conditions. The opposite situation is during Modoki II phase - any wave activity is absent already in the second half of February. Canonical winters demonstrate weak wave activity in the first decade of March or there is no any activity at all. But that’s beyond the scope of this paper.

Declarations

Author Contributions:

TE designed the research, wrote the paper and performed the analysis. AK developed software packages for calculating the RMC. AP helped to design and interpret the manuscript. SS, CW, and WK provided valuable suggestions to the interpretation of obtained results. All authors have seen, discussed and approved this version of the manuscript.

Acknowledgement:

MEI indices have been kindly provided by The NOAA Physical Sciences Laboratory, https://psl.noaa.gov/enso/mei/. This research was performed with a support of the grants from Russian Science Foundation #19-17-00198 and Russian Foundation for Basic Research #20-55-53039. RMS was studied at the Russian State Hydrometeorology University under the state task of the Ministry of Science and Higher Education of the Russian Federation (project FSZU-2020-0009). WC and KW are supported by National Natural Science Foundation of China (Grant #42011530082).

References

1. Ashok K, Behera SK, Rao SA, Weng H, Yamagata T (2007) El Niño Modoki and its possible teleconnections. J Geophys Res 112:C11007. https://doi.org/10.1029/2006JC003798
2. Andrews DG, McIntyre ME (1976) Planetary Waves in Horizontal and Vertical Shear: The Generalized Eliassen-Palm Relation and the Mean Zonal Acceleration. *J Atmos Sci* **33**:2031–2048. https://doi.org/10.1175/1520-0469(1976)033<2031:PWIHAV>2.0.CO;2
3. Bell CJ, Gray LJ, Charlton-Perez AJ, Joshi MM, Scaife AA (2009) Stratospheric communication of El Niño teleconnections to European winter. J Clim 22:4083– 4096. https://doi.org/10.1175/2009JCLI2717.1
4. Capotondi, A, Wittenberg AT, Newman M, Di Lorenzo E, Yu J-Y, Braconnot P, Cole J, Dewitte B, Giese B, Guilyardi E, Jin F-F, Karnauskas K, Kirtman B, Lee T, Schneider N, Xue Y, Yeh S-W (2015) Understanding ENSO Diversity. *Bull Amer Meteor Soc* **96:**921–938. https://doi.org/10.1175/BAMS-D-13-00117.1.
5. Chapman S, Lindzen RS (1970) Atmospheric Tides: Thermal and Gravitational. Gordon and Breach New York 200 pp. https://doi.org/10.1007/978-94-010-3399-2
6. Charney JG, Drazin PG (1961) Propagation of planetary-scale disturbances from the lower into the upper atmosphere. J Geophys Res 66(1): 83– 109. https://doi.org/10.1029/JZ066i001p00083
7. Chen W, Graf HF, Takahashi M (2002) Observed interannual oscillations of planetary wave forcing in the Northern Hemisphere winter. Geophys Res Lett 29:2073. https://doi.org/10.1029/2002GL016062
8. Chung CTY, Power SB (2017) The non-linear impact of El Niño, La Niña and the Southern Oscillation on seasonal and regional Australian precipitation. J South Hemisphere Earth Syst Sci 67(1):25-45. https://doi.org/10.22499/3.6701.003
9. Di Lorenzo E, Cobb KM, Furtado JC, Schneider N, Anderson BT, Bracco A, Alexander MA, Vimont DJ (2010) Central Pacific El Niño and decadal climate change in the North Pacific Ocean. Nat Geosci 3:762–765. https://doi.org/10.1038/ngeo984
10. Dima IM, Wallace JM (2007) Structure of the annual-mean equatorial planetary waves in the ERA-40 reanalyses. J At Sci 64(8):2862–2880. https://doi.org/10.1175/JAS3985.1
11. Domeisen DI, Garfinkel C, Butler AH (2019) The teleconnection of El Niño southern oscillation to the stratosphere. Rev Geophys 57:5–47. https://doi.org/10.1029/2018RG000596
12. Ermakova TS, Aniskina OG, Statnaia IA, Motsakov MA, Pogoreltsev AP (2019) Simulation of the ENSO influence on the extra-tropical middle atmosphere. Earth Planets Space 71:8. https://doi.org/10.1186/s40623-019-0987-9
13. Fedulina IN, Pogoreltsev AI, Vaughan G (2004) Seasonal, interannual and short-term variability of planetary waves in Met Office stratospheric assimilated fields. Quart J Roy Met Soc 130(602):2445–2458. https://doi.org/10.1256/qj.02.200
14. Foley A, Kelman I (2020) Precipitation responses to ENSO and IOD in the Maldives: Implications of large-scale modes of climate variability in weather-related preparedness. International. Journal of Disaster Risk Reduction 50:101726. https://doi.org/10.1016/j.ijdrr.2020.101726
15. Forbes JM, Hagan ME, Zhang X, Hamilton K (1997) Upper atmosphere tidal oscillations due to latent heat release in the tropical troposphere. Annals of Geophysics 15:1165-1175. https://doi.org/10.1007/s00585-997-1165-0

16. Garcia-Herrera R, Calvo N, Garcia RR, Giorgietta MA (2006) Propagation of ENSO temperature signals into the middle atmosphere: A comparison of two general circulation models and ERA-40 reanalysis data. J Geophys Res 111:6101–6115. https://doi.org/10.1029/2005JD006061
17. Garfinkel CI, Hartmann DL (2007) Effects of the El Niño–Southern Oscillation and the Quasi-Biennial Oscillation on polar temperatures in the stratosphere. J Geophys Res 112:D19112. https://doi.org/10.1029/2007JD008481
18. Garfinkel C I, Hartmann DL (2008) Different ENSO teleconnections and their effects on the stratospheric polar vortex. J Geophys Res 113:D18114. https://doi.org/10.1029/2008JD009920
19. Garfinkel CI, Hartmann DL, Sassi F (2010) Tropospheric precursors of anomalous northern hemisphere stratospheric polar vortices. J Clim 23(12): 3282–3299. https://doi.org/10.1175/2010JCLI3010.1
20. Holton JR, Mass C (1976) Stratospheric Vacillation Cycles. *J Atmos Sci* **33**:2218–2225. https://doi.org/10.1175/1520-0469(1976)033<2218:SVC>2.0.CO;2.
21. Hurwitz MM, Calvo N, Garfinkel CI, Butler AH, Ineson S, Cagnazzo C, Manzini E, Peña-Ortiz C (2014) Extra-tropical atmospheric response to ENSO in the CMIP5 models. Clim Dyn 43: 3367-3376. https://doi.org/10.1007/s00382-014-2110-z
22. Ineson S, Scaife A (2009) The role of the stratosphere in the European climate response to El Nino. Nature Geoscience 2:32-36. https://doi.org/10.1038/ngeo381
23. Iqbal A, Hassan SA (2018) ENSO and IOD analysis on the occurrence of floods in Pakistan. Nat Hazards 91:879–890. https://doi.org/10.1007/s11069-017-3158-y
24. Kao HY, Yu JY (2009) Contrasting eastern Pacific and central Pacific types of ENSO. J Clim 22:615–632. https://doi.org/10.1175/2008JCLI2309.1
25. Kim K-Y, Kim YY (2002) Mechanism of Kelvin and Rossby waves during ENSO events. Meteorol Atmos Phys 81:169–189. https://doi.org/10.1007/s00703-002-0547-9
26. Kug JS, Jin FF, An S-I (2009) Two types of El Niño events: Cold tongue El Niño and arm pool El Niño. J Clim 22:1499–1515. https://doi.org/10.1175/2008JCLI2624.1
27. Larkin NK, Harrison DE (2005) On the definition of El Niño and associated seasonal average U.S. weather anomalies. Geophys Res Lett 32(13):L13705. https://doi.org/10.1029/2005GL022738
28. Nobre GG, Jongman B, Aerts J, Ward P J (2017) The role of climate variability in extreme floods in Europe. Environmental Research Letters 12(8). https://doi.org/10.1088/1748-9326/aa7c22
29. Pogoreltsev AI, Fedulina IN, Mitchell NJ, Muller HG, Luo Y, Meek CE, Manson AH (2002) Global free oscillations of the atmosphere and secondary planetary waves in the MLT region during August/September time conditions. Journal of Geophysical Research 107. https://doi.org/10.1029/2001JD001535
30. Pogoreltsev AI, Vlasov AA, Fröhlich K, Jacobi Ch (2007) Planetary waves in coupling the lower and upper atmosphere. J Atmos Solar-Terr Phys 69:2083–2101. https://doi.org/10.1016/j.jastp.2007.05.014
31. Pogoreltsev AI, Kanukhina AY, Suvorova EV., Savenkova EN (2009) Variability of planetary waves as a signature of possible climatic changes. Journal of Atmospheric and Solar - Terrestrial Physics 71(14):1529-1539. https://doi.org/10.1016/j.jastp.2009.05.011

32. Power K, Barnett J, Dickinson T, Axelsson J (2020) The Role of El Niño in Driving Drought Conditions over the Last 2000 Years in Thailand. Quaternary 3(2):18. https://doi.org/10.3390/quat3020018
33. Qu T, Yu JY, (2014) ENSO indices from sea surface salinity observed by Aquarius and Argo. J Oceanogr 70:367–375. https://doi.org/10.1007/s10872-014-0238-4
34. Rakhman S, Lubis SW, Setiawan S (2017) Impact of ENSO on seasonal variations of Kelvin Waves and mixed Rossby-Gravity Waves. IOP Conference Series: Earth and Environmental Science 54:012035. https://doi.org/10.1088/1755-1315/54/1/012035
35. Rao J, Ren R (2016) A decomposition of ENSO's impacts on the northern winter stratosphere: competing effect of SST forcing in the tropical Indian Ocean. Clim Dyn 46:3689–3707. https://doi.org/10.1007/s00382-015-2797-5
36. Salby ML (1984) Survey of Planetary-Scale Traveling Waves: The State of Theory and Observations. Rev Geophys 22:209–236. https://doi.org/10.1029/RG022i002p00209
37. Smith KL, Fletcher CG, Kushner PJ (2010) The role of linear interference in the annular mode response to extratropical surface forcing. J Clim 23:6036–6050. https://doi.org/10.1175/2010JCLI3606.1
38. Smith KL, Kushner PJ (2012) Linear interference and the initiation of extratropical stratosphere–troposphere interactions. J Geophys Res 117:D13107. https://doi.org/10.1029/2012JD017587
39. Sung MK, Kim BM, An SI (2014) Altered atmospheric responses to Eastern Pacific and Central Pacific El Niños over the North Atlantic region due to stratospheric interference. Clim Dyn 42(1–2):159–170. https://doi.org/10.1007/s00382-012-1661-0
40. Taguchi, M, Hartmann DL (2006) Increased occurrence of stratospheric sudden warming during El Niño as simulated by WACCM. J Clim 19:324– 332. https://doi.org/10.1175/JCLI3655.1
41. Takahashi K, Montecinos A, Goubanova K, Dewitte B (2011) ENSO regimes: Reinterpreting the canonical and Modoki El Niño. Geophys Res Lett 38:L10704 https://doi.org/10.1029/2011GL047364
42. Torrence C, Compo G P (1998) A Practical Guide to Wavelet Analysis. Bull Amer Meteor Soc 79:61–78. https://doi.org/10.1175/1520-0477(1998)079<0061:APGTWA>2.0.CO;2
43. Tsuda T, Kato S (1989) Diurnal non-migrating tides excited by a differential heating due to land-sea distribution. Journal of the Meteorological Society of Japan 67:43-54. https://doi.org/10.2151/jmsj1965.67.1_43
44. Wang X, Wang C (2014) Different impacts of various El Niño events on the Indian Ocean Dipole. Climate Dyn **42:**991–1005. https://doi.org/10.1007/s00382-013-1711-2
45. Ward P J, Kummu M, Lall U (2016) Flood frequencies and durations and their response to El Niño Southern Oscillation: Global analysis. Journal of Hydrology 539:358-378. https://doi.org/10.1016/j.jhydrol.2016.05.045
46. Yeh SW, Kug JS, Dewitte B, Kwon M-H, Kirtman BP, Jin F-F (2009) El Niño in a hanging climate. Nature 461:511–514. https://doi.org/10.1038/nature08316
47. Yu J-Y, Kim ST (2011) Relationships between extratropical sea level pressure variations and the central Pacific and eastern Pacific types of ENSO. J Clim 24:708–720. https://doi.org/10.1175/2010JCLI3688.1.

Figures

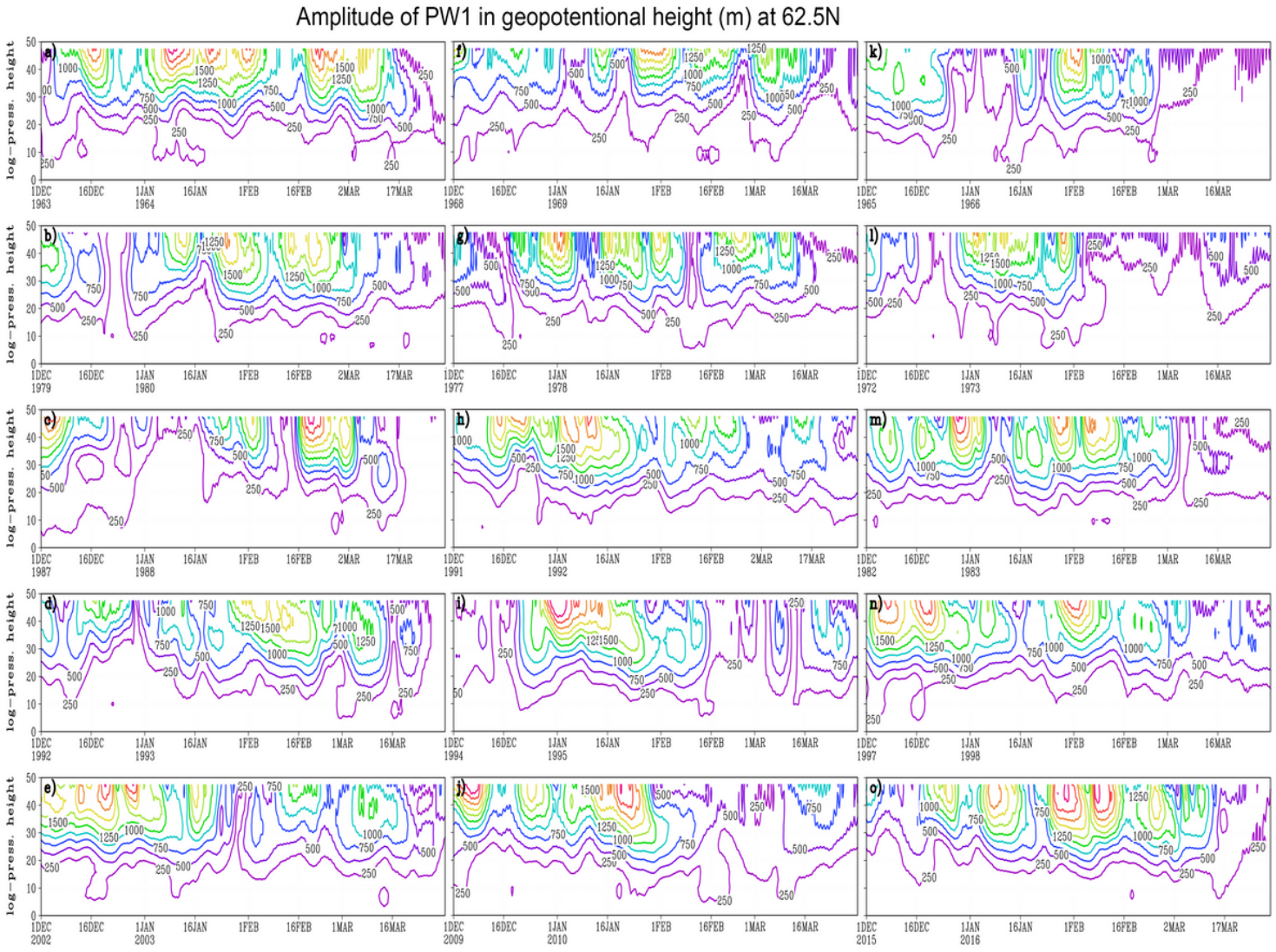

Figure 1

Amplitudes of planetary wave with zonal wave number 1 in geopotential height (meters) at 62.5°N. Winters during Modoki I conditions (a-e), Modoki II conditions (f-j), and canonical conditions (k-o)

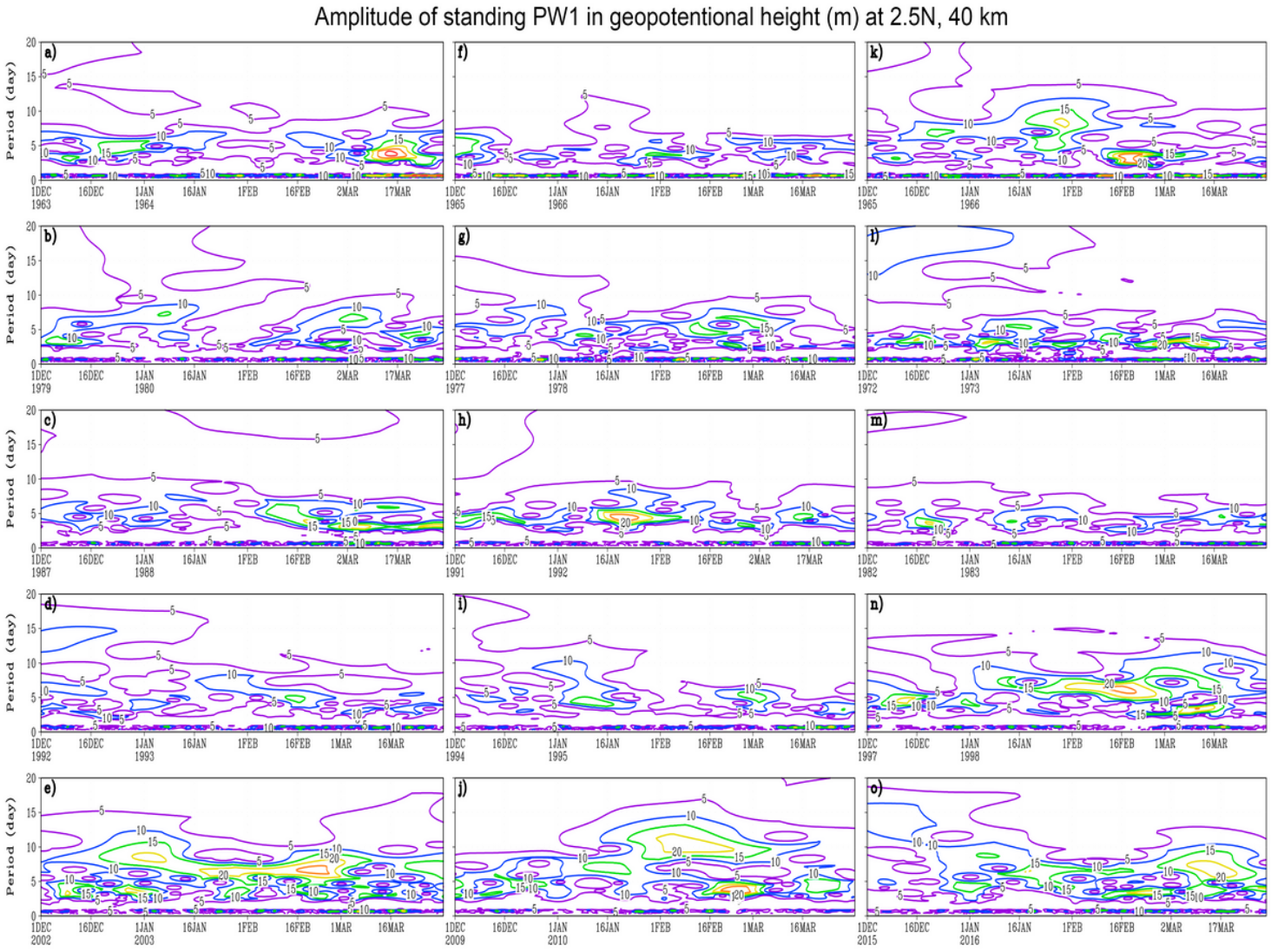

Figure 2

Amplitudes of standing planetary wave with zonal wave number 1 in geopotential height (meters) at 2.5°N, 40 km. Winters during Modoki I conditions (a-e), Modoki II conditions (f-j), and canonical conditions (k-o)

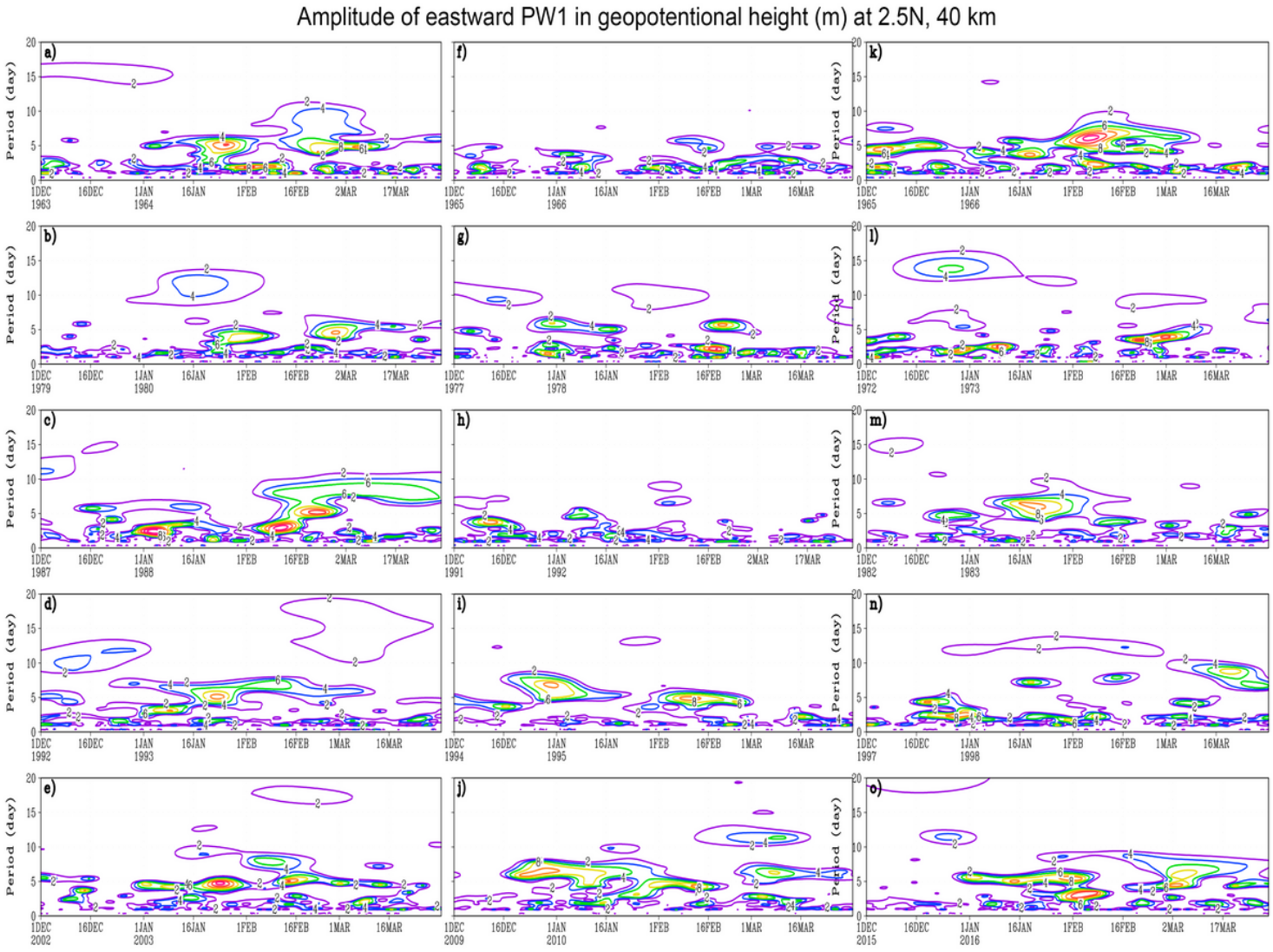

Figure 3

As in Fig. 2 but for the amplitudes of eastward propagating planetary waves

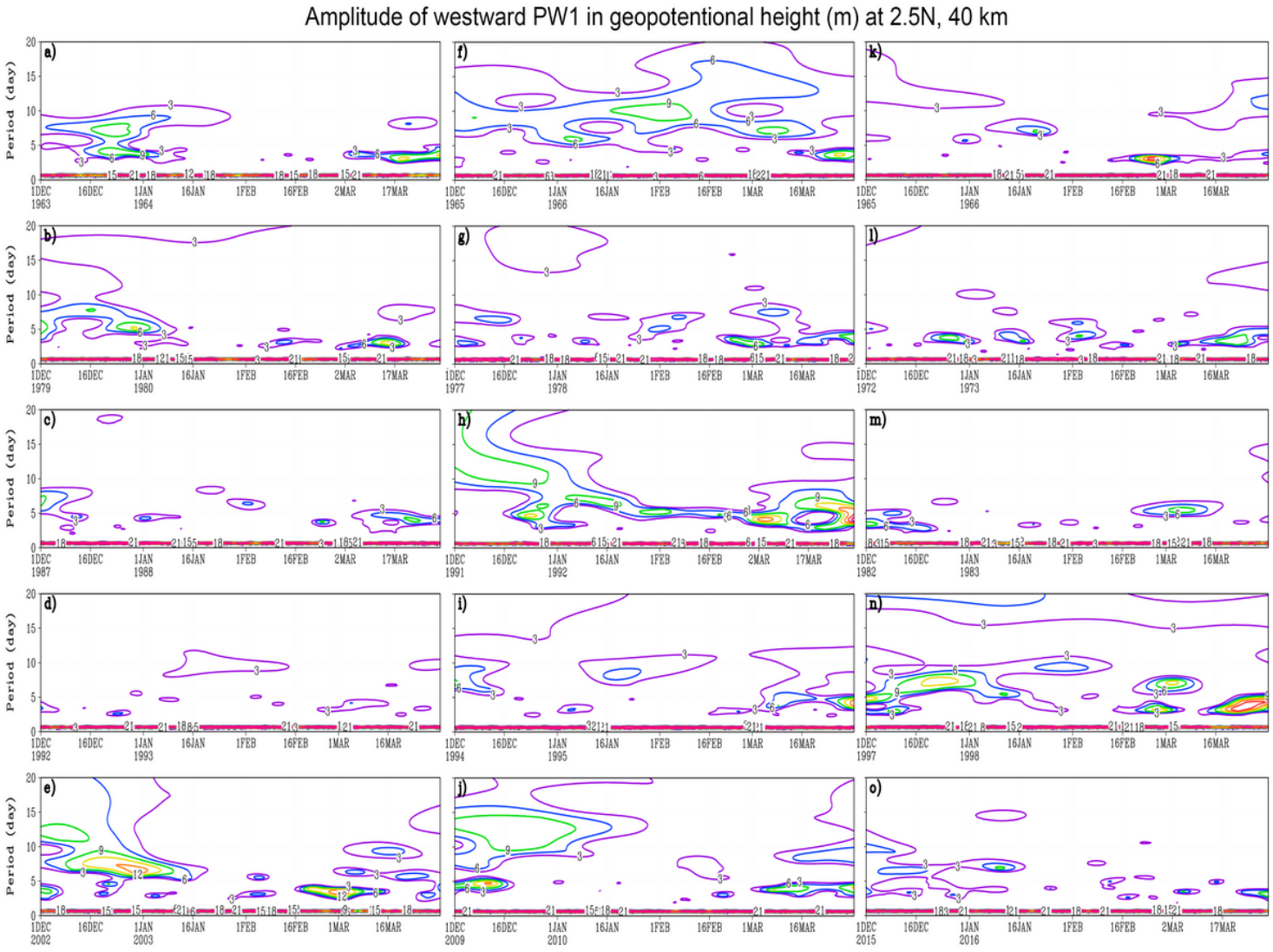

Figure 4

As in Fig. 2 but for the amplitudes of westward propagating planetary waves

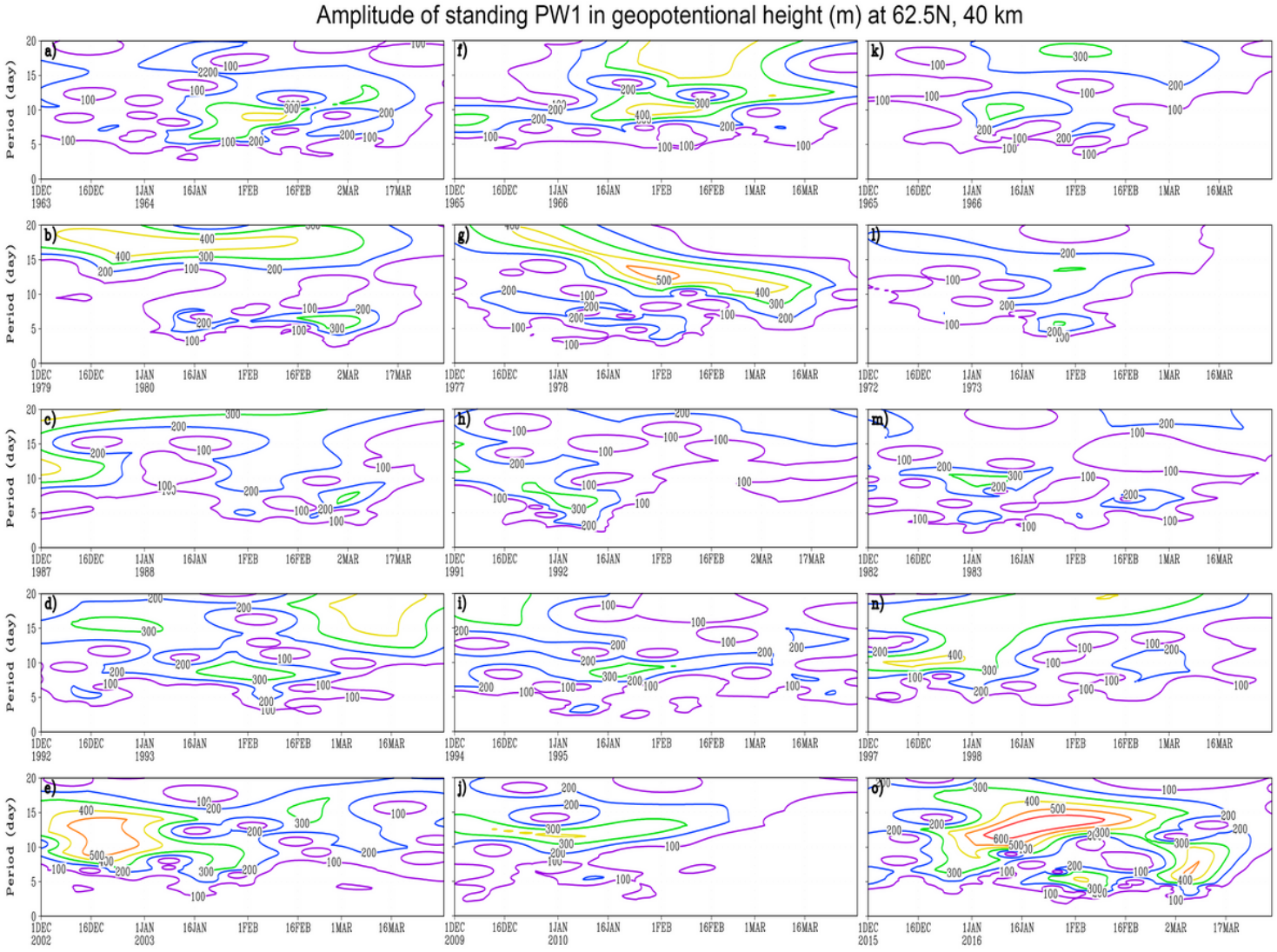

Figure 5

Amplitudes of standing planetary wave activity with zonal wave number 1 in geopotential height (meters) at 62.5°N, 40 km. Winters during Modoki I conditions (a-e), Modoki II conditions (f-j), canonical conditions (k-o)

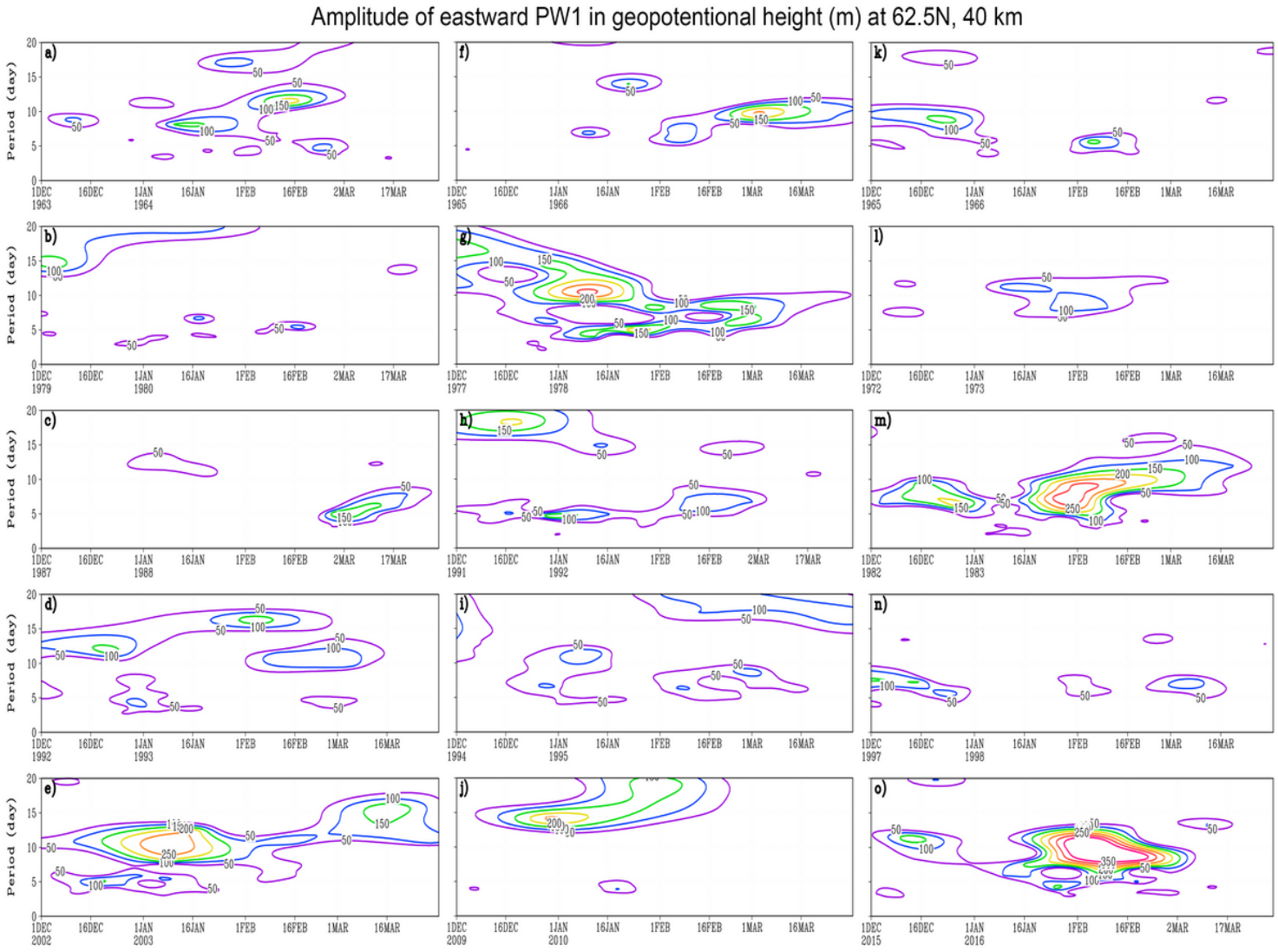

Figure 6

As in Fig. 5 but for the amplitudes of eastward propagating planetary waves

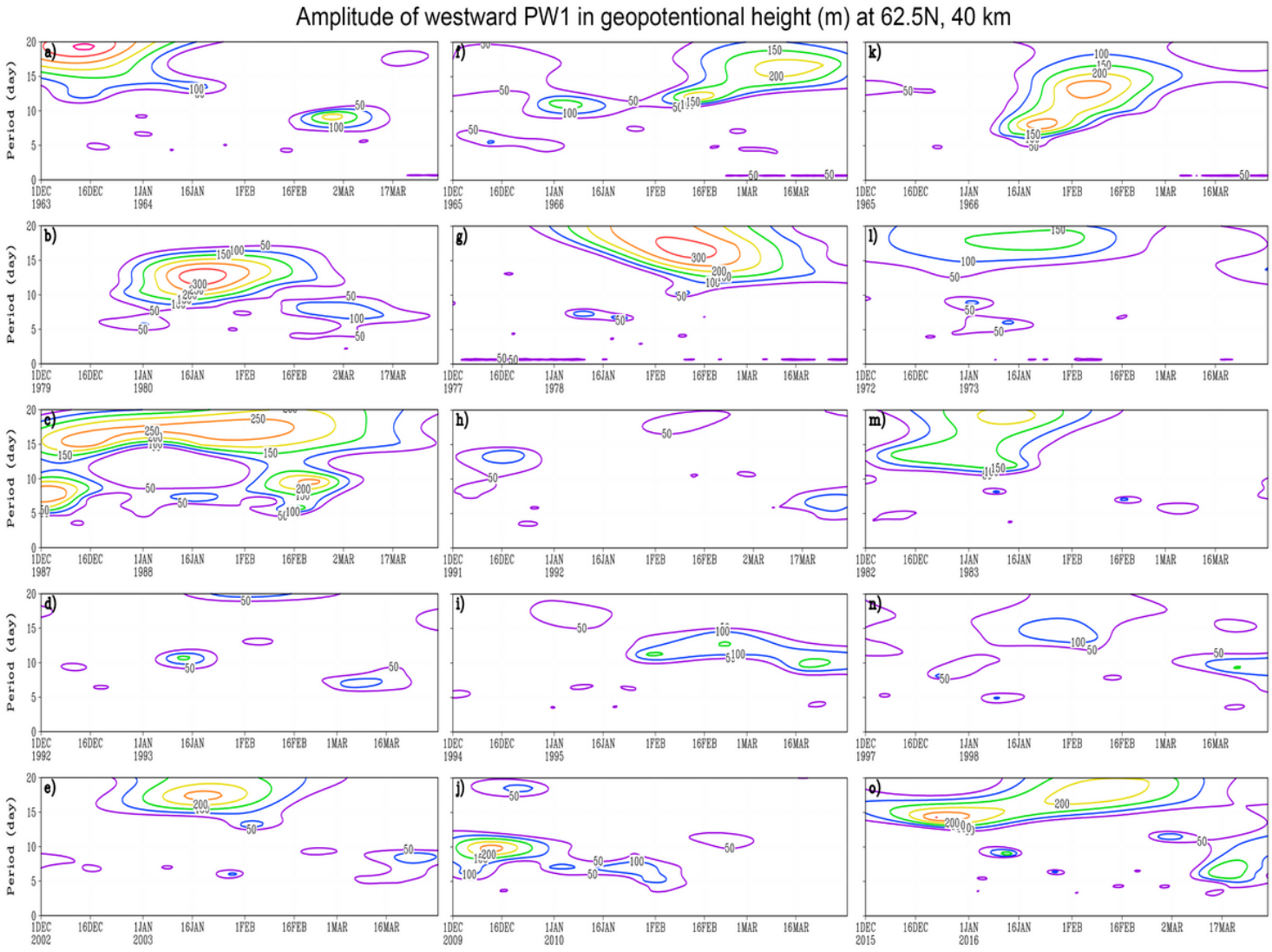

Figure 7

As in Fig. 5 but for the amplitudes of westward propagating planetary waves

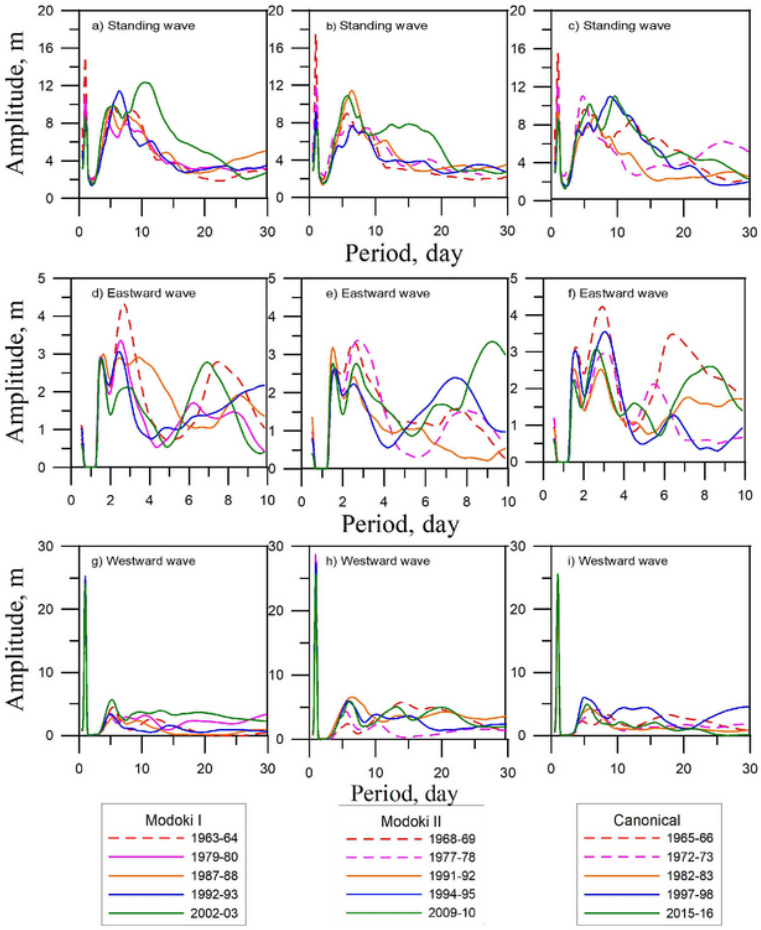

Figure 8

Figure 8 Standing waves (a-c), eastward waves (d-f), and westward waves (g-i) averaged over 5 months (from November to March) during Modoki I (a, d, g), Modoki II (b, e, h), canonical El Nino (c, f, i) at 2.5°N. The dashed curves correspond to the wave amplitudes observed in winters till 1979

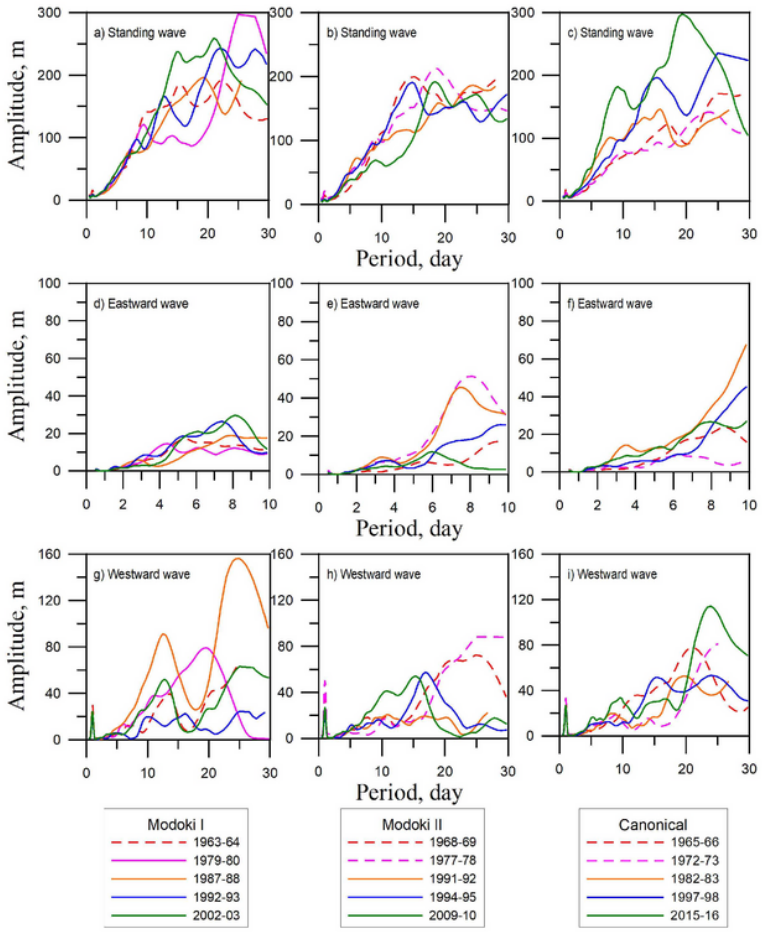

Figure 9

As in Fig. 8 but at 62.5°N

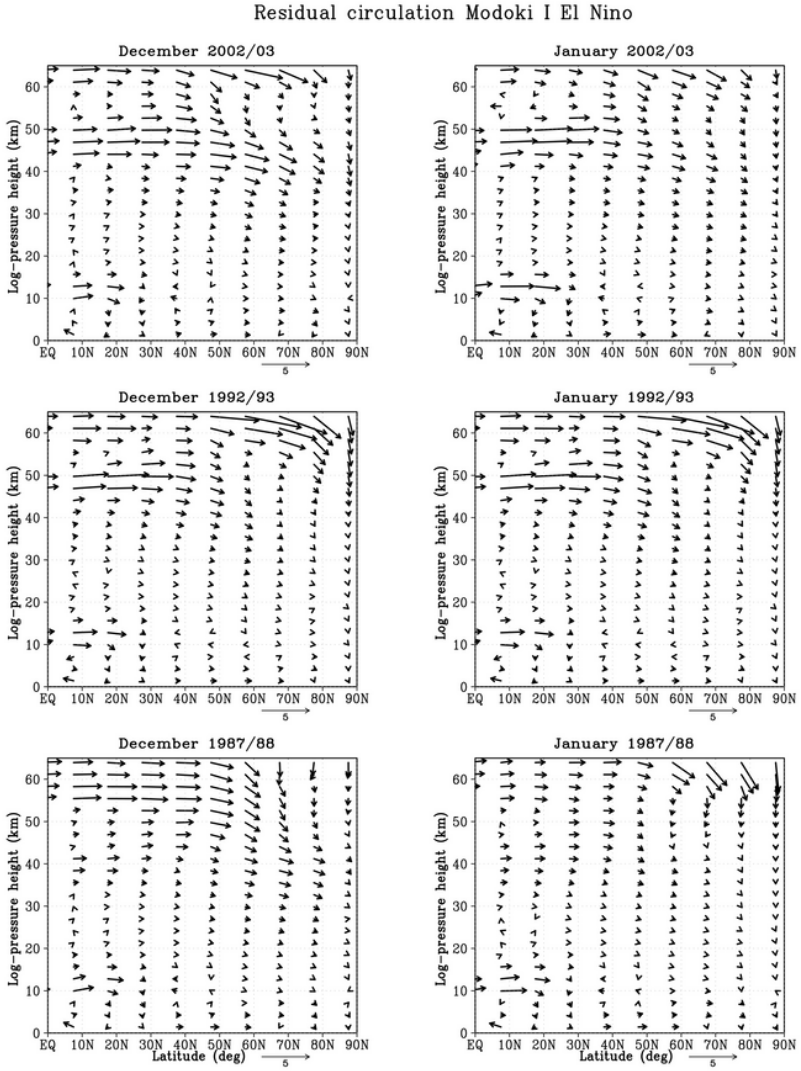

Figure 10

Monthly averaged residual meridional circulation in December (left panels) and January (right panels) during Modoki I El Nino event

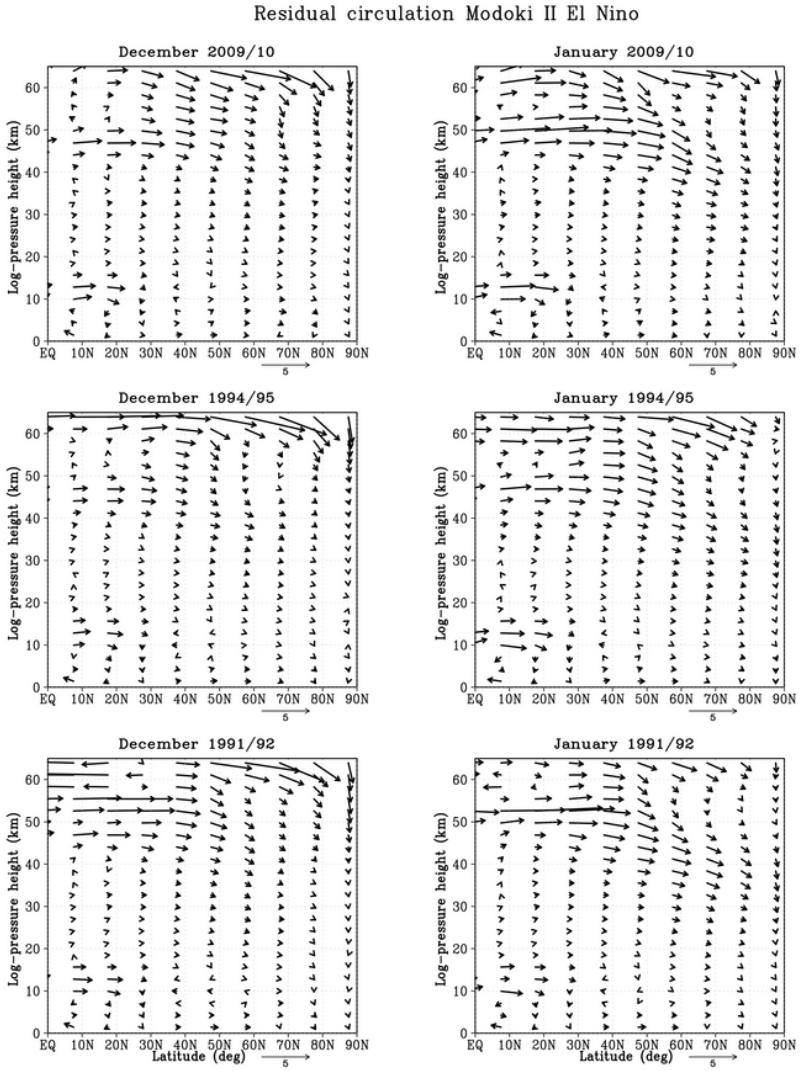

Figure 11

As in Fig. 11 but during Modoki II El Nino event

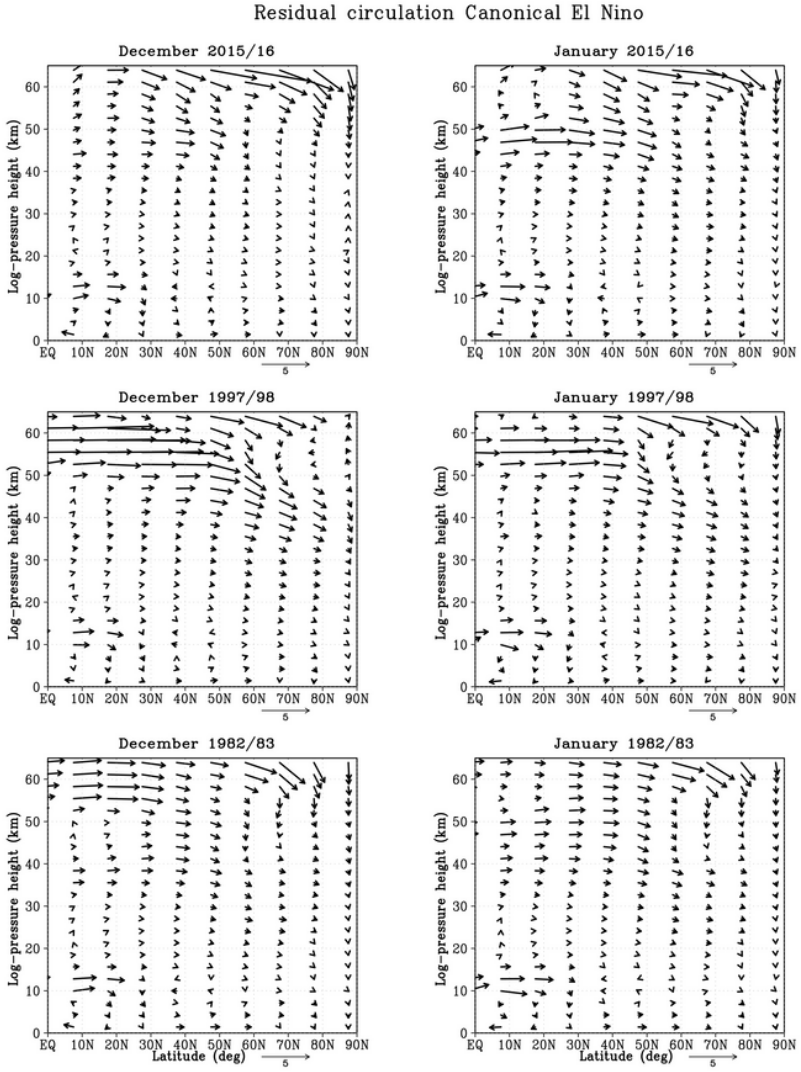

Figure 12

As in Fig. 11 but during canonical El Nino event